RSC Advances

ROYAL SOCIETY OF CHEMISTRY

www.rsc.org/advances

Graphical abstract

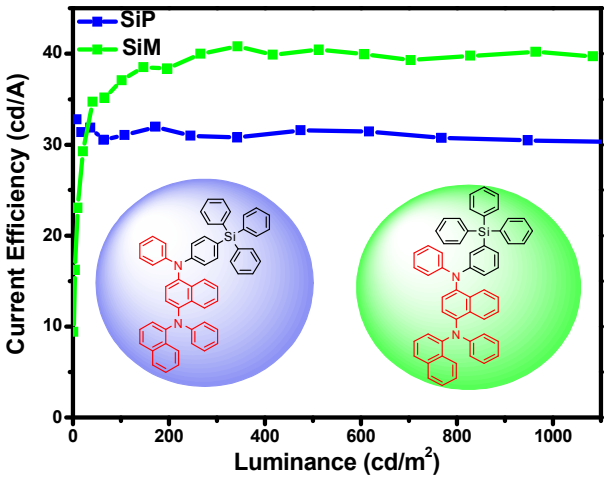

Two novel host materials **SiP** and **SiM** with high glass transition temperature were synthesized and yellow phosphorescent OLEDs show maximum current and power efficiency of 40.81 cd A^{-1} and 33.60 lm W^{-1} with low efficiency roll-off.

RSC Advances RSCPublishing

ARTICLE

Yellow electrophosphorescent devices with hosts containing N^1-(naphthalen-1-yl)-N^1,N^4-diphenylnaphthalene-1,4-diamine and tetraphenylsilane units

Song Zhang, Qiu-Lei Xu, Yi-Ming Jing, Xuan Liu, Guang-Zhao Lu, Xiao Liang, You-Xuan Zheng*, Jing-Lin Zuo

Cite this: DOI: 10.1039/x0xx00000x

Received 00th January 2012,
Accepted 00th January 2012

DOI: 10.1039/x0xx00000x

www.rsc.org/

Two novel host materials, N^1-(naphthalen-1-yl)-N^1,N^4-diphenyl-N^4-(4-(triphenylsilyl)phenyl) naphthalene-1,4-diamine (**SiP**) and N^1-(naphthalen-1-yl)-N^1,N^4-diphenyl-N^4-(3-(triphenylsilyl) phenyl)naphthalene-1,4-diamine (**SiM**), were synthesised by incorporating a hole-transporting moiety, N^1-(naphthalen-1-yl)-N^1,N^4-diphenylnaphthalene-1,4-diamine (**NPNA2**) and typical electron-transporting tetraphenylsilane moiety. **SiP** and **SiM** materials exhibit high thermal and morphological stability with high glass transition temperature higher than 110 °C and decomposition temperature above 350 °C. Using Ir(bt)$_2$(acac) (bis(2-phenylbenzothiozolato-N,$C^{2'}$)iridium(acetylacetonate)) as emitter, yellow phosphorescent organic light-emitting diodes of ITO/ TAPC (1,1-bis[4-(di-*p*-tolylamino)phenyl]cyclohexane, 40 nm)/ host : Ir(bt)$_2$(acac) (15 wt%, 20 nm)/ TmPyPB (1,3,5-tri(*m*-pyrid-3-yl-phenyl)benzene, 40 nm)/ LiF (1 nm)/ Al (100 nm) show maximum current and power efficiency of 40.81 cd A^{-1} and 33.60 lm W^{-1} with low efficiency roll-off. The current efficiency of 40.10 cd A^{-1} is still observed at the practically useful brightness value of 1000 cd m^{-2}.

Introduction

Organic light-emitting diodes (OLEDs) have been available on the market for over a decade and it is now a multi-billion dollar industry-mostly from touch-enabled active-matrix OLED (AMOLED) displays for mobile phones. In 1998, phosphorescent OLEDs (PHOLEDs) were first reported by Ma and Forrest et al.[1] In contrast to typical fluorescent OLEDs, PHOLEDs have attracted considerable attention because they can reach to 100% of theoretical internal quantum efficiency by harvesting both singlet and triplet excitons.[1,2] In PHOLEDs, to reduce the quenching associated with the relatively long exciton lifetimes, long diffusion lengths of triplet emitters and triplet-triplet annihilation, phosphorescent emitters of heavy-metal complexes are usually doped into a suitable host material.[3] It is desirable that the host materials ought to have a large enough triplet energy gap for efficient energy transfer to the guest, good carrier transport properties for a balanced recombination of holes and electrons in the emitting layer, energy-level matching with neighboring layers for effective charge injection[4] and high thermal and morphological stability. Among many design concepts for host materials, bipolar host materials have been the subject of interest because these materials have well-balanced charge transport properties that could extend the recombination zone, improve the device efficiency and simplify the device structure.[5] The incorporation of hole-transporting (donor) and electron-transporting (acceptor) moieties into the multifunctional host materials has been proved to be an efficient method to obtain bipolar small molecules. However, the conjugation caused by intramolecular donor-acceptor interactions may lower the triplet energies of bipolar molecules. Therefore, the development of the bipolar host possessing high triplet energy is still interesting for practical application. One of strategies adopted to suppress the donor-acceptor interactions for confining the triplet energy on the emitting phosphors is to introduce a π-conjugated bridge with a twisted conformation, which can partially reduce the electronic coupling of the donor and acceptor in the ground state. More efficiently, the incorporation of saturated centers such as sp^3-C or Si as the molecular bridge can usually block the electronic interactions between the hole-transporting and electron-transporting substructures.[4] Silicon atoms are used in host materials due to many advantages, such as conjugation blocking for a wide band gap and a tetrahedral geometry for morphology.[6]

The dimer of the *N*-phenyl-1-naphthylamine, N^1-(naphthalen-1-yl)-N^1,N^4-diphenylnaphthalene-1,4-diamine (**NPNA2**, E_T = 2.67 eV, low temperature photoluminescence spectra shown in Fig. S1), has ever been characterized to have high triplet energy, excellent hole-transporting ability and high thermal stability. Our previous research also demonstrated the successful utilization of the dimer of *N*-phenyl-1-naphthylamine as an effective electron-donating moieties in hole-transporting layer.[7] In the case of that, we adopted the hole-transporting moiety to two new silicon-based host materials, N^1-(naphthalen-1-yl)-N^1,N^4-diphenyl-N^4-(4-(triphenylsilyl)phenyl) naphthalene-1,4-diamine (**SiP**) and N^1-(naphthalen-1-yl)-N^1,N^4-diphenyl-N^4-(3-(triphenylsilyl)phenyl)naphthalene-1,4-diamine (**SiM**) by introducing triphenylsilane to the *para*- and *meta*-positions of a phenyl linker (Scheme 1). The triplet energy of the two host materials was almost the same because it is determined by the novel hole-transporting moiety **NPNA2**, which is higher than a widely used yellow phosphor of Ir(bt)$_2$(acac) (bis(2-phenylbenzothiozolato-

N,*C*$^{2'}$)iridium(acetylacetonate)),[8] and efficient energy transfer from the host materials to the Ir(bt)$_2$(acac) is expected.

Results and discussion

Synthesis and thermal property

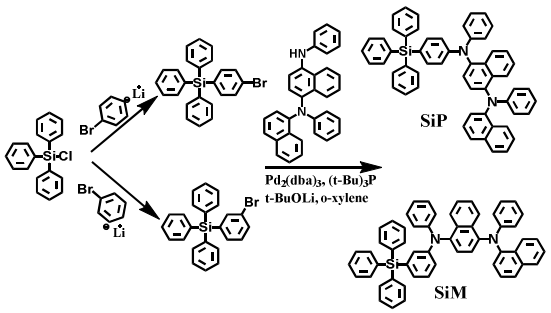

Scheme 1. Synthetic routes of **SiP** and **SiM**.

Scheme 1 shows the synthetic routes and structures of **SiP** and **SiM**. 1,4-Dibromobenzene and 1,3-dibromobenzene were sequentially treated with *n*-butyl-lithium and chlorotriphenylsilane to obtain (4-bromophenyl) triphenylsilane and (3-bromophenyl) triphenylsilane, respectively. Buchwald-Hartwig crossing-coupling of both organic halides with N^1-(naphthalen-1-yl)-N^1,N^4-diphenylnaphthalene-1,4-diamine (**NPNA2**) gave **SiP** and **SiM** with yields higher than 65%.

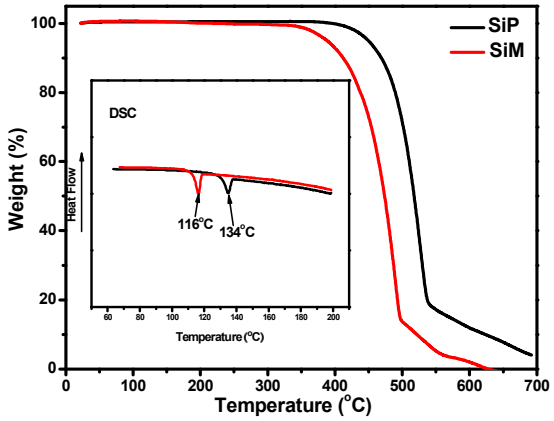

Fig. 1 TG curves of **SiP** (black line) and **SiM** (red line). Inset: DSC curves of **SiP** (black line) and **SiM** (red line).

The thermal property of host material is very important for stable OLEDs. The thermal gravimetric analysis (TGA) and differential scanning calorimetry (DSC) curves of **SiP** and **SiM** under a nitrogen atmosphere were listed in Fig. 1. Both compounds exhibit good thermal stabilities and the decomposition temperatures (T_d), which correspond to a 5% weight loss upon heating during TGA, were measured as 397 and 351 °C for **SiP** and **SiM**, respectively. And their corresponding glass transition temperatures (T_g) are 134 and 116 °C, respectively. The T_g values of the new compounds are much higher than those of the most reported bipolar hosts, such as the analogous silane-modified UGHs which had undesired low glass transition temperature in the range of 26-53 °C.[9] The high T_g values of these host materials may be mainly attributed to the configuration of the dimer of the *N*-phenylnaphthalen-1-amine, which can suppress intermolecular aggregation and improve the film morphology. The high T_d and T_g values of **SiP** and **SiM** are expected to decrease the phase separation rate of the guest-host system upon heating and have the potential use in high performance devices fabricated by vacuum thermal evaporation technology.[10]

Photophysical and electrochemical property

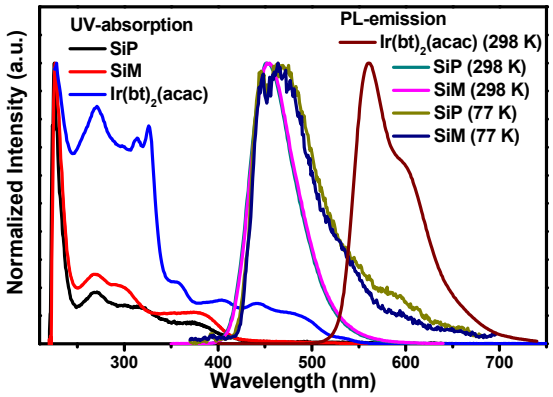

Fig. 2 UV-vis spectra of **SiP**, **SiM** and Ir(bt)$_2$(acac) in dichloromethane solution at room temperature; photoluminescence spectra in dichloromethane solution at 298 K of **SiP**, **SiM** and Ir(bt)$_2$(acac); phosphorescence spectra in dichloromethane solution glass matrix of **SiP** and **SiM** at 77 K.

The absorption spectra of **SiP**, **SiM** and Ir(bt)$_2$(acac) were tested in dichloromethane solution (Fig. 2). The absorption at 268 nm is attributed to the **NPNA2**-centered n-π* transition. The longer wavelength absorption observed at 378 nm for **SiP** and 381 nm for **SiM** are attributed to the the π-π* transitions from the electron-donating **NPNA2** moiety to the electron-accepting tetraphenylsilane moiety. The absorption bands of (bt)$_2$Ir(acac) at 441 and 481 nm are belong to the absorption transition from ground state to singlet ^{1}MLCT and triplet ^{3}MLCT excited state.[11] The photoluminescence spectra of **SiP**, **SiM** host materials and Ir(bt)$_2$(acac) at room temperature or 77 K are also shown in Fig 2. The maximum emission peak of Ir(bt)$_2$(acac) located at 560 nm with a slight shoulder at 597 nm. The emission peaks of **SiP** and **SiM** at room temperature are 452 and 451 nm, respectively, suggesting the position of triphenylsilane on phenyl linker has negligible effect on the emission. There is a good overlap between the fluorescence bands of two novel hosts and the MLCT absorption of Ir(bt)$_2$(acac), suggesting a possible energy transfer from **SiP** and **SiM** to Ir(bt)$_2$(acac). The triplet energies of the **SiP** and **SiM** were determined as 2.64 and 2.67 e V, respectively, from the highest energy vibronic sub-band of their phosphorescence spectra at 77 K (Table 1). From their triplet alignments, it also can be speculated that there should be an efficient energy transfer from host triplet states to the Ir(bt)$_2$(acac) triplet states and an excellent triplet energy confinement on the Ir(bt)$_2$(acac) molecules within the emissive layers.

Table 1. Photophysical data of compounds **SiP** and **SiM.**

Compound	T_d/T_g [a] (°C)	Absorption [b] λ (nm)	Emission λ_{em}(nm) [b] 298 K	E_T [c] (eV)	HOMO (eV)	LUMO (eV)
SiP	397/134	268/378	452	2.64	-5.19	-2.31
SiM	351/116	268/381	451	2.67	-5.18	-2.27

[a] T_g: Glass transition temperatures, T_d: decomposition temperatures. [b] Measured in dichloromethane solution at room temperature. [c] triplet energy: estimated from the highest-energy peaks of the 77 K phosphorescence spectra.

The redox properties and highest occupied molecular orbital (HOMO), lowest unoccupied molecular orbital (LUMO) energy levels of the hosts are relative to the charge transport ability and the OLED structure. For evaluation the HOMO/LUMO energy levels, the electrochemical properties of **SiP** and **SiM** were probed by cyclic voltammetry (CV) using ferrocene as the internal standard (Fig. S2). The hosts exhibited two reversible oxidation and reduction behaviors, which were most likely resulting from the electrochemical properties of the **NPNA2** moiety. The oxidation potentials of **SiP** and **SiM** were found at 0.392 and 0.382 V versus Ag/Ag^+, respectively. According to the equation $E_{HOMO} = -(E_{ox}^{onset} + 4.8)$ eV,[12] the HOMO levels of **SiP** and **SiM** were estimated to be approximately -5.19 and -5.18 eV, respectively, which is about 0.31 and 0.32 eV higher than that of TAPC (5.50 eV),[13] and thus theoretically barrier-free hole injection from the hole-transport layer can be realized.[14] The corresponding LUMO levels calculated from the HOMO values and the band gaps (2.88 and 2.91 eV) were found to be approximately -2.31 and -2.27 eV, respectively.

OLEDs performance

To compare the charge-transporting properties of **SiP** and **SiM**, the current density - voltage (*J* - *V*) characteristics of hole-only devices (**HOD**) with the configuration ITO/ host (30 nm)/ TAPC (1,1-bis[4-(di-*p*-tolylamino)phenyl]cyclohexane, 60 nm)/ Al (100 nm) and electron-only devices (**EOD**) with the configuration ITO/ TmPyPB (1,3,5-tri(*m*-pyrid-3-yl-phenyl)benzene, 60 nm)/ host (60 nm)/ LiF (1 nm)/ Al (100 nm) were investigated. The TAPC or TmPyPB layer was used to prevent electron- or hole-injection from cathode or anode, respectively. In general, asymmetric substitution at the *meta*-position would be an effective strategy for the design of high-performance bipolar host materials.[15] However, **HODs** and **EODs** showed two hosts were not found obvious bipolar characters because the hole current density is two orders of magnitude higher than the electron current density (Fig. 3). These results demonstrate that the hole transport properties of **NPNA2**-based electron-donating moiety is much better than the electron transport properties of tetraphenylsiliane-based electron-withdrawing moiety. Furthermore, **SiP** and **SiM** exhibit negligible differences of electron mobility (Fig. 3(b)). But the hole transport ability of **SiP** is little higher than that of **SiM** at same driving voltages. Considering the similar physical properties of two compounds, the slightly different carrier-transporting properties between **SiP** and **SiM** are probably due to their different steric configurations.

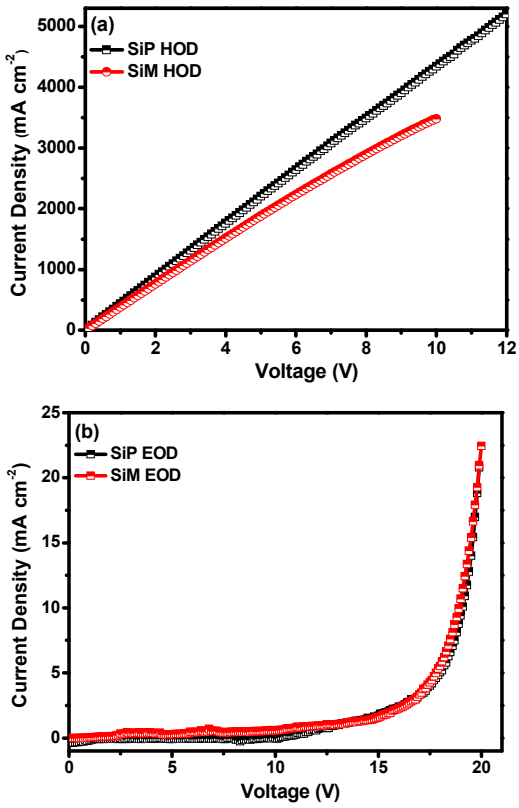

Fig. 3 Current density-voltage of hole-only (a) and electron-only (b) devices made of **SiP** and **SiM**.

Using the traditional multilayer device configuration ITO/ TAPC (40 nm)/ host : $Ir(bt)_2(acac)$ (15 wt%, 20 nm)/ TmPyPB (40 nm)/ LiF (1 nm)/ Al (100 nm), we investigated the function of **SiP** and **SiM** as hosts. The molecule structures and energy level diagrams of the materials and devices are shown in Fig. 4. TAPC and TmPyPB were used as the hole- and electron-transporting layers, respectively. $Ir(bt)_2(acac)$ was used as the phosphor emitter with the optimized doping concentration of 15 wt%, which is a little higher than common yellow devices.[16] This may be attributed to the LUMO level of $Ir(bt)_2(acac)$ (-2.95 eV) which was significantly lower than that of two hosts, electrons had the potential to be trapped at $Ir(bt)_2(acac)$. At higher doping level, more electrons were injected directly to the dopant molecules, which provided an additional channel to transport electrons through hopping between the dopant sites.[17] Accordingly, higher dopant concentration such as 15 wt%

improved the charge balance and energy transfer from host to guest. Though the HOMO level of $Ir(bt)_2(acac)$ (-5.29 eV) is lower than that of **SiP** and **SiM**, there is near no energy barrier for the hole transport from TAPC to dopant and hosts due to the higher HOMO level of TAPC (Fig. 4).

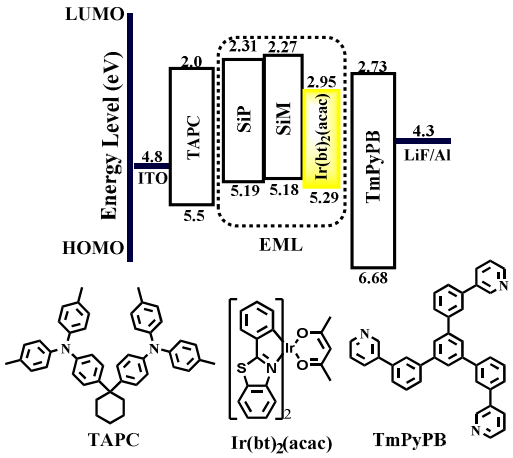

Fig. 4 Energy level diagram of yellow PHOLEDs and molecular structures of materials used.

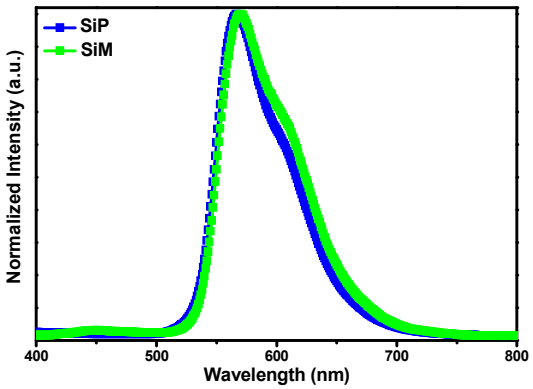

Fig. 5 Electroluminescence spectra measured at 8.0 V.

The electroluminescence (EL) spectra of the devices are listed in Fig. 5; the current density-voltage-luminance (*J* - *V* - *L*), current efficiency-luminance (η_c - *L*) and power efficiency-luminance (η_p - *L*) curves are shown in Fig. 6. The key device performance parameters are summarized in Table 2. The EL spectra of the **SiP**- and **SiM**-based yellow PHOLEDs showed a main peak at 563 or 565 nm and a slight shoulder peak appeared at 595 nm from $Ir(bt)_2(acac)$. There is no peak origin from **SiP** and the emission from **SiM** are very weak. This suggests that the emission peaks are indeed derived from the dopant, and the triplet energy transfer from the hosts to the dopant are nearly complete. The Commission Internationale de l'Eclairage (CIE) color coordinates of the **SiP**- and **SiM**-based devices are (0.49, 0.48) and (0.51, 0.47), respectively.

Both **SiP**- and **SiM**-based devices have low turn-on voltages of 2.9 V at a luminance of 1 cd m^{-2}. The main reason for such low turn-on voltage is the relative high HOMO energy levels of the two hosts and there is no barrier against a hole transport from TAPC into **SiP** or **SiM**. The low LUMO of $Ir(bt)_2(acac)$ and 15 wt% doped concentration also lowered the energy loss for the electron transport from TmPyPB to the emissive layer. As anticipated from the charge-transporting ability results, the device using **SiP** as host show higher current density than **SiM**-based device (Fig. 6(a)). From Fig. 6(b) it can be observed that the **SiM**-based device has a maximum current efficiency of 40.81 cd A^{-1} and a maximum external quantum efficiency (EQE) of 15.1% at a luminance of 343.01 cd m^{-2} with mild efficiency roll-off. At the practical luminance of 1000 cd m^{-2}, the current efficiency of 40.10 cd A^{-1} can be obtained. Even at the luminance of 10000 cd m^{-2}, a current efficiency around 32 cd A^{-1} still can be maintained. As a result of the low driving voltage, the **SiM** device also shows maximum power efficiency of 33.60 lm W^{-1}.

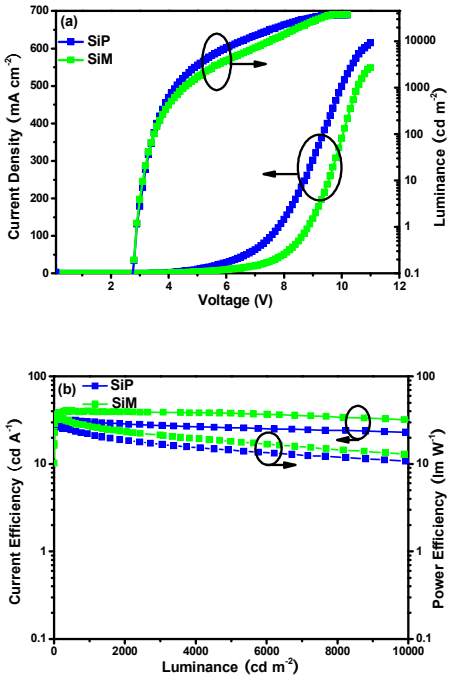

Figure 6. (a) Current density-voltage-luminance (*J* - *V* - *L*); (b) current efficiency-luminance (η_c - *L*) and power efficiency-luminance (η_p - *L*) characteristics of the PHOLEDs with **SiP** and **SiM**.

On the other hand, the efficiencies of **SiP**-based device (a maximum current efficiency $\eta_{c,max}$ of 31.96 cd A^{-1}, a maximum external quantum efficiency EQE of 11.10% and a maximum power efficiency $\eta_{p,max}$ of 30.79 lm W^{-1}) were slightly lower than that of the **SiM**-based device. This result can be understood by considering the hole- and electron-transport properties of two hosts. It should be noted that the hole mobility of TAPC (hole mobility (μ_h) $\approx 10^{-2}$ cm^2 v^{-1} s^{-1})[18] is higher than the electron mobility of TmPyPB (electron mobility (μ_e) $\approx 10^{-3}$ cm^2 v^{-1} s^{-1})[19] and in this case, the hole-trapping recombination mechanism may affects the efficiencies of the devices. More imbalance of holes and electrons injection will cause more serious hole-trapping in the emitting layer. At the low current density, hole-trapping could provide an additional emission process and will improve the efficiency.[20] However, the more trapped holes

will lead to triplet-polaron quenching and induce the efficiency roll-off when the current density increased.[21] Therefore, the relative low hole mobility and more balanced carriers in the **SiM**-based device could lead to a relatively higher utilization ratio of the carriers in the emissive layer, resulting in the higher efficiency.

Table 2. Electroluminescence performances of the devices based on **SiP** and **SiM**.

Host	$V_{turn\text{-}on}$ [a]	L_{max} (voltage)[b]	$\eta_{c,max}$(luminance) [c]	$\eta_{c,L1000}$ [d]	$\eta_{p,max}$ [e]	EQE_{max} [f]	CIE [g]
	(V)	[cd m^{-2} (V)]	[cd A^{-1}(cd m^{-2})]	(cd A^{-1})	[lm W^{-1}]	(%)	(x,y)
SiP	2.9	36731(10.0)	31.96(172.09)	30.30	30.79	11.10	0.49,0.48
SiM	2.9	37768(10.2)	40.81(343.01)	40.10	33.60	15.10	0.51,0.47

[a] $V_{turn\text{-}on}$: Turn-on voltage recorded at a luminance of 1 cd m^{-2}; [b] L_{max}: maximum luminance; [c] $\eta_{c,max}$: maximum current efficiency; [d] $\eta_{c,L1000}$: current efficiency at 1000 cd m^{-2}; [e] $\eta_{p,max}$: maximum power efficiency; [f] EQE_{max}: maximum external quantum efficiency; [g] Measured at 8 V.

Conclusions

In conclusion, two novel host materials **SiP** and **SiM** have been synthesized by attaching the N^1-(naphthalen-1-yl)-N^1,N^4-diphenylnaphthalene-1,4-diamine moiety to the triphenylsilane segment *via* the *para*- and *meta*-position of the *N*-phenyl. Both compounds exhibit good thermal stabilities with glass transition temperatures of 134 and 116 °C, respectively. The host materials have sufficient triplet energy (E_T > 2.6 eV) for good energy transfer to yellow phosphor $Ir(bt)_2(acac)$. In traditional multilayer structures, a device with **SiP** as a host achieved maximum $\eta_{c,max}/\eta_{p,max}$ of 31.96 cd A^{-1}/30.79 lm W^{-1} and **SiM**-based device achieved maximum $\eta_{c,max}/\eta_{p,max}$ of 40.81 cd A^{-1}/33.60 lm W^{-1}. This study indicates that the new hole-transporting moiety is an excellent unit for building host materials for efficient yellow PHOLEDs.

Experimental

Materials and measurements.

^{1}H NMR and ^{13}C NMR spectra were measured on a Bruker AM 500 spectrometer and a Bruker AM 126 spectrometer, respectively. Mass spectra (MS) were obtained with MALDI-TOF (Bruker Daltonic Inc.). High resolution mass spectra (Agilent 6540 UHD Accurate-Mass Q-TOF LC/MS) were recorded for the compounds. TGA and DSC measurements were carried out on STA 449F3 (NETZSCH) and 823e (METTLER), respectively. Absorption and emission spectra were measured on a Shimadzu UV-3100 and a Hitachi F-4600 luminescence spectrophotometer, respectively. The low temperature phosphorescence spectra were measured with an Edinburgh Instruments FLS-920 spectrophotometer at 77 K. Cyclic Volta metric experiments were carried out with an CHI 600E system (Chenhua, Shanghai) using three electrode cell assemblies in deaerated dichloromethane solution with tetrabutylammoniumperchlorate as supporting electrolyte at a scan rate of 100 mV s^{-1}. Each oxidation potential was calibrated with ferrocene as a reference.

OLEDs fabrication and measurement.

Organic chemicals used for OLEDs were generally purified by high-vacuum, gradient temperature sublimation. The devices were fabricated by vacuum deposition of the materials at 10^{-6} Torr onto a ITO (indium tin oxide) glass substrate (a sheet resistance of 15 Ω square^{-1}) with a deposition rate of 1-2 Å s^{-1}. The phosphor and host were co-evaporated to form 20 nm emitting layer from two separate sources. The LiF and Al were deposited with deposition rates of 0.1 and 3 Å s^{-1}, respectively. The characteristics of the devices were measured with a computer controlled KEITHLEY 2400 source meter with a calibrated silicon diode in air without device encapsulation. The CIE coordinates were calculated using a testing program of the Spectra scan PR650 spectrophotometer.

Syntheses.

All reactions were performed under nitrogen. Solvents were carefully dried and distilled from appropriate drying agents prior to use for syntheses of ligands. **NPNA2** was synthesised according to our previous report.[7]

4-Bromophenyltriphenylsilane. 12.5 mL of a 1.6 M solution of *n*-BuLi (20 mmol) in hexane is added dropwise to a solution of 4.72 g, 3.027 ml (20 mmol) of 1,4-dibromobenzene in 100 ml of ether at -78 °C. Then the mixture is allowed to warm up to ambient temperature within 2.5 h. The mixture is again cooled to -78 °C and 5.90 g of chlorotriphenylsilane (20 mmol, resolved in ether) is added in a dropwise manner. After warming the mixture to ambient temperature and stirring overnight the solvent is removed in vacuo and the residue was purified by column chromatography on silica gel using n-hexane as the eluent to give a white powder. Yield: 75%. MS (MALDI-TOF, *m/z*) Calcd for $C_{24}H_{19}SiBr$: 414.044. Found: 413.949 $[M]^+$.

3-Bromophenyltriphenylsilane. 3-Bromophenyltriphenylsilane was prepared according to the same procedure as compound 4-bromophenyltriphenylsilane but 1,3-dibromobenzene instead of 1,4-dibromobenzene was used as a starting material. Yield: 72%. MS (MALDI-TOF, *m/z*) Calcd for $C_{24}H_{19}SiBrNa^+$: 439.031. Found: 440.450 $[M+Na]^+$.

N^1-(Naphthalen-1-yl)-N^1,N^4-diphenyl-N^4-(4-(triphenylsilyl) phenyl)naphthalene-1,4-diamine (SiP). $Pd_2(dba)_3$ (0.09 g, 0.10 mmol), **NPNA2** (0.04 g, 1.0 mmol), Li^{t}BuO (0.32 g, 4.0 mmol), and (4-bromophenyl)triphenylsilane (0.50 g, 1.2 mmol) were added into a 50 mL two-neck flask. The flask was evacuated and backfilled

with nitrogen. *o*-xylene (20 mL) and P^{t}Bu$_3$ (1.23 mL, 0.4 mmol, 10% in *n*-hexane) were injected. The mixture was heated at 140 °C for 48 h and extracted twice with CH_2Cl_2 at room temperature. The mixed organic solution was washed with brine and dried over anhydrous sodium sulfate. The solid obtained was purified with column chromatography on SiO_2 using ethyl acetate and petroleum ether (v : v = 1 : 50) as eluant to afford 0.51 g **SiP** (0.67 mmol, 67%). ^{1}H NMR (500 MHz, $CDCl_3$, Fig. S3) δ[ppm] 8.12 (d, *J* = 8.4 Hz, 1H), 8.08 (d, *J* = 8.5 Hz, 1H), 8.02 (d, *J* = 8.3 Hz, 1H), 7.91 (d, *J* = 8.2 Hz, 1H), 7.73 (d, *J* = 8.2 Hz, 1H), 7.60 - 7.54 (m, 6H), 7.51 - 7.47 (m, 1H), 7.42 (dd, *J* = 7.5, 3.8 Hz, 3H), 7.40 - 7.34 (m, 11H), 7.27 - 7.22 (m, 5H), 7.17 (dd, *J* = 15.6, 7.6 Hz, 5H), 6.99 (d, *J* = 8.4 Hz, 3H), 6.89 (d, *J* = 7.3 Hz, 1H), 6.77 (d, *J* = 7.6 Hz, 2H). ^{13}C NMR (126 MHZ, $CDCl_3$, Fig. S5) δ[ppm] 150.44, 149.65, 147.57, 144.70, 143.51, 140.33, 137.32, 136.42, 135.28, 134.75, 132.89, 131.68, 130.30, 129.50, 129.25, 129.05, 128.55, 127.84, 126.66, 126.51, 126.34, 126.21, 126.11, 125.85, 125.38, 125.15, 125.12, 124.84, 124.78, 124.44, 123.01, 122.63, 120.78, 120.40, 119.54. HR EI-MS (*m/z*) Calcd for $C_{56}H_{42}N_2Si$: 770.3117. Found: 770.3115 $[M]^+$ (Fig. S7). IR (KBr, cm^{-1}, Fig. S9): 3131.80, 1585.93, 1492.32, 1458.88, 1394.12, 1282.60, 1108.21, 768.86, 700.51, 517.02.

***N*^{1}-(Naphthalen-2-yl)-*N*^{1},*N*^{4}-diphenyl-*N*^{4}-(3-(triphenylsilyl) phenyl)naphthalene-1,4-diamine (SiM)**. Compound **SiM** was prepared according to the same procedure as compound **SiP** but (3-bromophenyl)triphenylsilane instead of (4-bromophenyl) triphenylsilane was used as a starting material. Yield: 65%. ^{1}H NMR (500 MHz, $CDCl_3$, Fig. S4) δ[ppm] 8.13 - 8.08 (m, 1H), 8.06 (d, *J* = 8.5 Hz, 1H), 8.02 - 7.96 (m, 1H), 7.91 (d, *J* = 8.2 Hz, 1H), 7.72 (d, *J* = 8.1 Hz, 1H), 7.48 - 7.46 (m, 6H), 7.39 - 7.35 (m, 5H), 7.34 (dd, *J* = 5.7, 3.9 Hz, 3H), 7.31 (s, 2H), 7.25 - 7.21 (m, 3H), 7.20 (d, *J* = 4.4 Hz, 3H), 7.17 (d, *J* = 7.3 Hz, 3H), 7.10 (dd, *J* = 12.6, 7.3 Hz, 4H), 7.04 (d, *J* = 7.9 Hz, 3H), 6.90 (dd, *J* = 17.0, 7.5 Hz, 3H), 6.71 (d, *J* = 7.9 Hz, 2H). () ^{13}C NMR (126 MHz, $CDCl_3$, Fig. S6) δ[ppm] 150.43, 148.29, 147.69, 144.70, 143.14, 140.79, 136.28, 135.27, 135.05, 134.15, 132.64, 131.70, 130.25, 129.74, 129.70, 129.53, 129.06, 129.01, 128.81, 128.52, 127.82, 127.52, 126.47, 126.41, 126.28, 126.21, 126.08, 125.75, 125.35, 125.07, 124.96, 124.44, 123.19, 121.53, 121.45, 120.66, 120.34. HR EI-MS (*m/z*) Calcd for $C_{56}H_{42}N_2Si$: 770.3117. Found: 770.3122 $[M]^+$. (Fig. S8) IR (KBr, cm^{-1}): 3132.19, 3063.67, 1584.75, 1487.75, 1459.44, 1392.49, 1282.24, 1108.03, 769.60, 744.19, 701.22, 510.40 (Fig. S10).

Acknowledgements

This work was supported by the National Natural Science Foundation of China (21371093, 91433113), the Major State Basic Research Development Program (2011CB808704, 2013CB922101) and the Natural Science Foundation of Jiangsu Province (BK20130054).

Notes and References

State Key Laboratory of Coordination Chemistry, Collaborative Innovation Center of Advanced Microstructures, School of Chemistry and Chemical Engineering, Nanjing University, Nanjing 210093, P. R. China, e-mail: yxzheng@nju.edu.cn

†Electronic Supplementary Information (ESI) available. For the photoluminescence spectra of **NPNA2** in dichloromethane solution at 298 and 20 K, cyclic voltammograms of **SiP** and **SiM** in dichloromethane solution see DOI:10.1039/b000000x/.

References

1 (*a*) Y. G. Ma, H. Y. Zhang, J. C. Shen and C. M. Che, *Synth. Met.,* 1998, **94**, 245; (*b*) M. A. Baldo, D. F. O'Brien, Y. You, A. Shoustikov, S. Sibley, M. E. Thompson and S. R. Forrest, *Nature.,* 1998, **395**, 151.

2 (*a*) P.-T. Chou and Y. Chi, *Chem. -Eur. J.,* 2007, **13**, 380; (*b*) Y. Chi and P.-T. Chou, *Chem. Soc. Rev.,* 2010, **39**, 638; (*c*) L. Xiao, Z. Chen, B. Qu, J. Luo, S. Kong, Q. Gong and J. Kido, *Adv. Mater.,* 2011, **23**, 926; (*d*) C.-H. Fan, P. Sun, T.-H. Su and C.-H. Cheng, *Adv. Mater*., 2011, **23**, 2981; (*e*) H.-H. Chou, Y.-K. Li, Y.-H. Chen, C.-C. Chang, C.-Y. Liao, and C.-H. Cheng, *ACS Appl. Mater. Interfaces*, 2013, **5**, 6168; (*f*) X. Xu, X. Yang, J. Dang, G. Zhou, Y. Wu, H. Li and W.-Y. Wong, *Chem. Commun*., 2014, **50**, 2473; (*g*) X. Yang, G. Zhou and W.-Y. Wong, *J. Mater. Chem. C*, 2014, **2**, 1760.

3 W. Jiang, L. Duan, J. Qiao, G. Dong, D. Zhang, L. Wang and Y. Qiu, *Dyes Pigments.,* 2012, **92**, 891.

4 (*a*) A. Chaskar, H. -F. Chen and K. T. Wong, *Adv. Mater.,* 2011, **23**, 3876. (*b*) S. -H. Chou, W. -Y. Hung, C. -M. Chen, Q.-Y. Liu, Y. -H. Liu and K. -T. Wong, *RSC Adv.,* 2013, **3**, 13891.

5 (*a*) K. S. Yook and J. Y. Lee, *Adv. Mater.,* 2012, **24**, 3169; (*b*) L. Duan, J. Qiao, Y. Sun and Y. Qiu, *Adv. Mater.,* 2011, **23**, 1137.

6 (*a*) W. -S. Han, H. -J. Son, K. -R. Wee, K. -T. Min, S. Kwon, Il-H. Suh, S. -H. Choi, D. -H. Jung and S. -O. Kang, *J. Phys. Chem. C.,* 2009, **113**, 19686; (*b*) R. J. Holmes, B. W. D'Andrade, S. R. Forrest, X. Ren, J. Li and M. E. Thompson, *Appl. Phys. Lett.,* 2003, **83**, 3818; (*c*) X. M. Liu, C. B. He, J. C. Huang and J. M. Xu, *Chem. Mater.,* 2005, **17**, 434; (*d*) X. -M. Liu, C. B. He, X. -T. Hao, L. -W. Tan, Y. Q. Li, K. S. Ong, *Macromolecules.,* 2004, **37**, 5965; (*e*) X. M. Liu, J. W. Xu, X. H. Lu and C. B. He, *Org. Lett.,* 2005, **7,** 2829; (*f*) D. -R. Bai and S. N. Wang, *Organometallics.,* 2004, **23**, 5958; (*g*) H. -C. Yeh, C. -H. Chien, P. -I Shih, M. -C. Yuan and C. -F. Shu, *Macromolecules.,* 2008, **41**, 3801; (*h*) S. -J. Yeh, M. -F. Wu, C. -T. Chen, Y. -H. Song, Y. Chi, M. -H. Ho, S. -F. Hsu and C. H. Chen, *Adv. Mater.,* 2005, **17**, 285; (*i*) M. -F. Wu, S. -J. Yeh, C. -T. Chen, H. Murayama, T. Tsuboi, W. -S. Li, I. Chao, S. -W. Liu and J. -K. Wang, *Adv. Funct. Mater.,* 2007, **17**, 1887; (*j*) M. -H. Tsai, H. -W. Lin, H. -C. Su, T. -H. Ke, C. -C. Wu, F. -C. Fang, Y. -L. Liao, K. -T. Wong and C. -I. Wu, *Adv. Mater.,* 2006, **18**, 1216; (*k*) J. -J. Lin, W. -S. Liao, H. -J. Huang, F. -I. Wu and C. -H. Cheng, *Adv. Funct. Mater.,* 2008, **18**, 485.

7 S. Zhang, L.-S. Xue, Y.-M. Jing, X. Liu, G.-Z. Lu, X. Liang, H.-Y. Li, Y.-X. Zheng, J.-L. Zuo, *Dyes Pigms*., 2015, DOI: 10.1016/j.dyepig.2015.02.011.

8 C. Fan, L. P. Zhu, B. Jiang, Y. -F. Li, F. -C. Zhao, D. -G. Ma, J. -G. Qin and C. -L. Yang, *J. Phys. Chem. C.,* 2013, **117**, 19134.

9 (*a*) P. -I. Shih, C. -H. Chien, C. -Y. Chuang, C. -F. Shu, C. -H. Yang, J. -H. Chen and Y. Chi, *J. Mater. Chem.,* 2007, **17**, 1692; (*b*) X. F. Ren, J. Li, R. J. Holmes, P. I. Djurovich, S. R. Forrest and M. E. Thompson, *Chem. Mater.,* 2004, **16**, 4743; (*c*) S. -L. Gong, Q. Fu, Q. Wang, C. -L. Yang, C. Zhong, J. -G. Qin and D.-G. Ma, *Adv. Mater.,* 2011, **23**, 4956.

10 C. -J. Zheng, J. Ye, M. -F. Lo, M. -K. Fung, X. -M. Ou, X. -H. Zhang and C. -S. Lee, *Chem. Mater.,* 2012, **24**, 643.

11 (*a*) X. Wei, J. Peng, J. Cheng, M. Xie, Z. Lu, C. Li and Y. Cao, *Adv. Funct. Mater.,* 2007, **17**, 3319; (*b*) S. M. Chen, G. P. Tan, W. -Y. Wong and H. -S. Kwok, *Adv. Funct. Mater.,* 2011, **21**, 3785.

12 (*a*) Q. Sun, H. Wang, C. Yang and Y. Li, *J. Mater. Chem.,* 2003, **13**, 800; (*b*) J. Pommerehne, H. Vestweber, W. Guss, R. F. Mahrt, H. Bassler, M. Porsch and J. Daub, *Adv. Mater.,* 1995, **7**, 551.

13 G. Liaptsis and K. Meerholz, *Adv. Funct. Mater.,* 2013, **23**, 359.

14 B.H Zhang, G. P. Tan, C. -S. Lam, B. Yao, C. -L. Ho, L. H. Liu, Z. Y. Xie, W. -Y. Wong, J. Q. Ding and L. X. Wang, *Adv. Mater.,* 2012, **24**, 1873.

15 M.-K. Yan, Y. Tao, R.-F. Chen, C. Zheng, Z.-F. An and W. Huang, *RSC Adv.,* 2012, **2**, 7860.

16 H. -F. Chen, T. -C. Wang, S. -W. Lin, W. -Y. Hung, H. -C. Dai, H. -C. Chiu, K. -T. Wong, M. -H. Ho, T. -Y. Cho, C. -W. Chen and C. -C. Lee, *J. Mater. Chem.,* 2012, **22**, 15620.

17 F. -M. Hsu, C. -H. Chien, P. -I. Shih and C. -F. Shu, *Chem. Mater.,* 2009, **21**, 1017.
18 Y. Miao, X. Du, H. Wang, H. Liu, H. Jia, B. Xu, Y. Hao, X. Liu, W. Li and W. Huang, *RSC Adv.,* 2014, **5**, 4261.
19 S.-J. Su, T. Chiba, T. Takeda and J. Kido, *Adv. Mater.,* 2008, **20**, 2125.
20 (*a*) C. Han, F. Zhao, Z. Zhang, L. Zhu, H. Xu, J. Li, D. Ma and P. Yan, *Chem. Mater.,* 2013, **25**, 4966; (*b*) F. Zhao, N. Sun, H. Zhang, J. Chen and D. J. Ma, *Appl. Phys.,* 2012, **112**, 084504; (*c*) Q. Wang, J. Ding, D. Ma, Y. Cheng, L. Wang, X. Jing and F Wang, *Adv. Funct. Mater.,* 2009, **19**, 84.
21 J. Jin, W. Zhang, B. Wang, G. Mu, P. Xu, L. Wang, H. Huang, J. Chen and D. Ma, *Chem. Mater.,* 2014, **26,** 2388.